# *Porphyromonas gingivalis* Promotes Colorectal Carcinoma by Activating the Hematopoietic *NLRP3* Inflammasome AC

Xi Wang[1], Yiqun Jia[1,2], Liling Wen[1], Wenxin Mu[1], Xianrui Wu[3], Tao Liu[4], Xiangqi Liu[1], Juan Fang[1], Yizhao Luan[5], Ping Chen[6], Jinlong Gao[7], Ky-Anh Nguyen[7], Jun Cui[4], Gucheng Zeng[8], Ping Lan[3], Qianming Chen[9], Bin Cheng[1], and Zhi Wang[1]

## ABSTRACT

*Porphyromonas gingivalis* (*P. gingivalis*) is a keystone periodontal pathogen associated with various digestive cancers. However, whether *P. gingivalis* can promote colorectal cancer and the underlying mechanism associated with such promotion remains unclear. In this study, we found that *P. gingivalis* was enriched in human feces and tissue samples from patients with colorectal cancer compared with those from patients with colorectal adenoma or healthy subjects. Cohort studies demonstrated that *P. gingivalis* infection was associated with poor prognosis in colorectal cancer. *P. gingivalis* increased tumor counts and tumor volume in the $Apc^{Min/+}$ mouse model and increased tumor growth in orthotopic rectal and subcutaneous carcinoma models. Furthermore, orthotopic tumors from mice exposed to *P. gingivalis* exhibited tumor-infiltrating myeloid cell recruitment and a proinflammatory signature. *P. gingivalis* promoted colorectal cancer via NLRP3 inflammasome activation *in vitro* and *in vivo*. NLRP3 chimeric mice harboring orthotopic tumors showed that the effect of NLRP3 on *P. gingivalis* pathogenesis was mediated by hematopoietic sources. Collectively, these data suggest that *P. gingivalis* contributes to colorectal cancer neoplasia progression by activating the hematopoietic NLRP3 inflammasome.

**Significance:** This study demonstrates that the periodontal pathogen *P. gingivalis* can promote colorectal tumorigenesis by recruiting myeloid cells and creating a proinflammatory tumor microenvironment.

**Graphical Abstract:** http://cancerres.aacrjournals.org/content/canres/81/10/2745/F1.large.jpg.

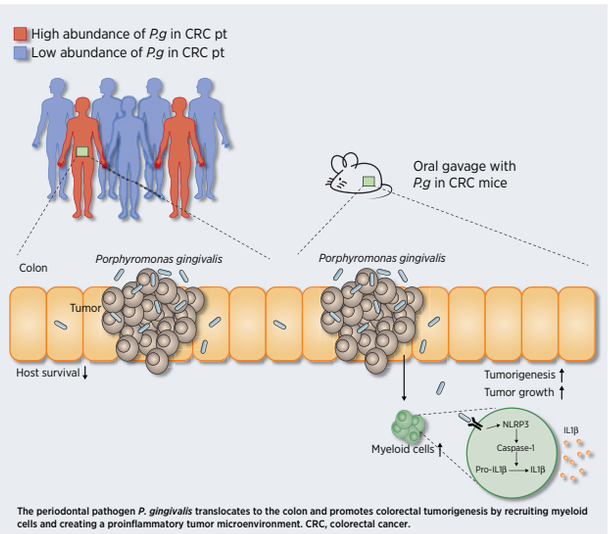


## Introduction

Gut microbiota homeostasis plays important roles in health and disease. In humans, diseases, particularly metabolic syndrome and obesity-related diseases, liver diseases, inflammatory bowel disease (IBD), and colorectal cancer can originate from dysbiosis of the gut microbiota in humans (1). The oral cavity harbors a complex microbiome. The lower part of the digestive tract is "inoculated" every day by more than 1,000 bacterial species from the oral cavity, and one study reported that the microbial species detected in the oral and fecal microbiota overlap in approximately 45% of tested individuals (2). The oral microbiome has been viewed as an important factor affecting gut

[1]Hospital of Stomatology, Guanghua School of Stomatology, Guangdong Provincial Key Laboratory of Stomatology, Sun Yat-sen University, Guangzhou, China. [2]Stomatology Center, Shenzhen People's Hospital, the Second Clinical Medical College of Jinan University, the First Affiliated Hospital of Southern University of Science and Technology, Shenzhen, China. [3]Department of Colorectal Surgery, Guangdong Provincial Key Laboratory of Colorectal and Pelvic Floor Diseases, Guangdong Institute of Gastroenterology, The Sixth Affiliated Hospital, Sun Yat-sen University, Guangzhou, China. [4]MOE Key Laboratory of Gene Function and Regulation, State Key Laboratory of Biocontrol, School of Life Sciences, Sun Yat-sen University, Guangzhou, China. [5]State Key Laboratory of Ophthalmology, Guangdong Provincial Key Lab of Ophthalmology and Visual Science, Zhongshan Ophthalmic Center, Sun Yat-sen University, Guangzhou, China. [6]Department of Gastroenterology, Affiliated Hospital of Inner Mongolia Medical University, Hohhot, China. [7]Institute of Dental Research, Sydney Dental School, Faculty of Medicine and Health, The University of Sydney, Sydney, New South Wales, Australia. [8]Zhongshan School of Medicine, Sun Yat-sen University, Guangzhou, China. [9]The Affiliated Hospital of Stomatology, and Key Laboratory of Oral Biomedical Research of Zhejiang Province, School of Stomatology, Zhejiang University School of Medicine, Hangzhou, Zhejiang, China.

**Note:** Supplementary data for this article are available at Cancer Research Online (http://cancerres.aacrjournals.org/).

X. Wang, Y. Jia, and L. Wen contributed equally to this article.

Corrected online April 28, 2022.

**Corresponding Authors:** Zhi Wang, Hospital of Stomatology, Sun Yat-sen University, No. 56 Lingyuan West Road, Guangzhou 510055, China. Phone: 8620-0591-8733; E-mail: wangzh75@mail.sysu.edu.cn; and Bin Cheng, chengbin@mail.sysu.edu.cn

Cancer Res 2021;81:2745–59

**doi:** 10.1158/0008-5472.CAN-20-3827

microbiota homeostasis in recent years (3). Recent studies have shown that the oral bacterium *Fusobacterium nucleatum* invades human epithelial cells and promotes the progression of colorectal adenomas via multiple potential mechanisms (4–7). *Porphyromonas gingivalis* (*P. gingivalis*) is also a gram-negative oral anaerobe that is involved in the pathogenesis of periodontitis (8). Recently, serum anti–*P. gingivalis* IgG antibodies were found to be associated with overall orodigestive cancer mortality (9), and *Porphyromonas* was reported to be enriched in feces from patients with colorectal cancer (10). Moreover, Rachel and colleagues also showed that *P. gingivalis* was associated with tumor consensus molecular subtypes (CMS), which are closely associated with colorectal cancer (11). However, evidence regarding the effects of *P. gingivalis* on promoting colorectal cancer tumorigenesis or development is lacking.

Exogenous substances such as pathogens can activate the innate immune response of hosts (12); the resulting signaling can cause profound inflammation. The three major classes of innate immune receptors include Toll-like receptors (TLR), retinoic acid–inducible gene I-like helicases (RIG-I-like helicases), and Nod-like receptor (NLR) proteins. NLRs are involved in the assembly of large protein complexes known as inflammasomes, which participate in the innate immune response to pathogens such as *P. gingivalis* (13). However, this surveillance machinery responds differently to *P. gingivalis* in different cell types and disease conditions (14–17). We explored the concept that the innate immune machinery, whose canonical function is the detection of pathogen-associated molecular patterns and other moieties from foreign organisms, may contribute to the development of colorectal cancer in mice due to activation driven by *P. gingivalis*.

In this study, we found that *P. gingivalis* from the oral cavity was enriched in tissue and fecal samples and that its abundance was positively associated with a poor prognosis in patients with colorectal cancer. Consistent with this observation, *P. gingivalis* promoted colorectal cancer tumorigenesis and progression in three different mouse tumor models. Colorectal cancer tumors contain myeloid-derived immune cells in the microenvironment, and immune cells restrict activation of the nucleotide-binding oligomerization domain receptor and pyrin domain containing 3 (NLRP3) inflammasome. Collectively, these data suggest that by recruiting tumor-infiltrating myeloid cells and activating the NLRP3 inflammasome, *P. gingivalis* generates a proinflammatory microenvironment that is conducive to the progression of colorectal neoplasms. Our study extends the knowledge of how the oral microbiota influences the processes involved in the colorectal inflammatory microenvironment and colorectal cancer.

## Materials and Methods

### Patients

The Sun Yat-sen University Institutional Review Board approved the use of human samples for this study. Fecal samples ($n = 77$) were provided by 22 subjects without colorectal diseases, 23 patients with colorectal cancer, and 32 patients with colorectal adenoma from the Affiliated Hospital of Inner Mongolia Medical University. Paired tissue samples (colorectal cancer tissue and adjacent normal tissue samples) from 31 subjects and 62 formalin-fixed paraffin-embedded (FFPE) samples (20 normal, 20 adenoma, and 22 colorectal cancer samples) were collected from the Sixth Affiliated Hospital of Sun Yat-sen University (Guangzhou, China). The above samples had limited sample sizes without recurrence and survival information.

We studied two cohorts of patients with colorectal cancer from the southern and northern parts of China enrolled between 2012 and 2018. There were 155 FFPE samples in cohort 1 from the Sixth Affiliated Hospital and Cancer Center of Sun Yat-sen University and 237 FFPE samples in cohort 2 from the Affiliated Hospital of Inner Mongolia Medical University. We used cohort 1 as the discovery cohort and cohort 2 as the validation cohort. The patients were pathologically diagnosed with colorectal cancer and over 18 years of age. Recurrence was monitored by pathological and clinical diagnosis.

### Human specimen collection

#### Colonic tumor samples and matched normal tissue samples

Patients were identified from upcoming operative cases by P. Chen in the Department of Gastroenterology, Affiliated Hospital of Inner Mongolia Medical University, and X. Wu in the Department of Colorectal Surgery, the Sixth Affiliated Hospital of Sun Yat-sen University. The inclusion criteria were patients who had biopsy-confirmed colorectal cancer and were undergoing hemicolectomy. Exclusion criteria included a known synchronous cancer diagnosis or other cancer diagnosis within 5 years of the operation and a history of IBD. No antibiotics were given preoperatively. Fresh colorectal cancer and adjacent nontumor tissues from each subject were collected. Samples were snap frozen in liquid nitrogen and then stored at −80°C until use. Written informed consent was obtained from all participants.

#### Colonic adenoma samples

Patients were identified, and samples were collected by a coinvestigator (X.Wu). Written informed consent was obtained from all participants.

#### Stool collection

Patients with scheduled colonoscopy at the Department of Gastroenterology, Affiliated Hospital of Inner Mongolia Medical University from 2014 to 2017 were included in the study. The indications for colonoscopy were gastrointestinal bleeding, weight loss, changes in bowel movements, or detection of polyps/tumors on CT colonography. No antibiotics were given preoperatively. Colon cancer was confirmed by biopsy; colonic adenoma was confirmed by colonoscopy. All samples were collected preoperatively. The patients were divided into three groups based on findings during colonoscopy: one group with colorectal cancer, one group with adenomatous polyps, and one control group without pathologic findings. Each patient collected a stool sample in RNAlater RNA Stabilization buffer (Qiagen) prior to bowel preparation or 1 week after colonoscopy. When samples arrived at the laboratory, they were homogenized and stored at −80 C. Written informed consent was obtained from each study participant.

### Animal care

All procedures were approved and performed in accordance with the guidelines of the Institutional Animal Care and Use Committee of Sun Yat-sen University (Guangzhou, China). *NLRP3*$^{-/-}$ C57BL/6J mice were provided by Professor Jun Cui, Sun Yat-sen University (Guangzhou, China). C57BL/6J-*Apc*$^{Min/+}$ mice and wild-type (WT) mice were ordered from the Model Animal Research Center of Nanjing University (Nanjing, China). All mice were maintained in the barrier facility at the Sun Yat-sen University Animal Center (Guangzhou, China).

### Colorectal adenoma mouse model

Forty C57BL/6J-*Apc*$^{Min/+}$ mice were divided into the *P. gingivalis* group, *S. mutans* group (negative control), and sham group (blank control). Bacterial feeding experiments were performed for a period of

8 weeks, beginning at 6 weeks of age. Bacteria were gavaged at a dosage of $10^8$ CFU two times per week. The sham treatment consisted of feeding BHI broth.

### Orthotopic and subcutaneous colorectal xenograft mouse model

An orthotopic rectal cancer model was generated in WT C57BL/6J mice as described previously (18). Briefly, MC38 cells were obtained from ATCC in 2016 and were tested for authentication and *Mycoplasma* contamination within 6 months. MC38 cells used were no more than 15 passages. The mice were injected with $5 \times 10^5$ MC38 cells at 6 weeks of age. Bacterial feeding experiments were performed for a period of 2 weeks, beginning at 7 weeks of age. Bacteria were gavaged at a dosage of $10^8$ CFU two times per week. MC38 cells ($5 \times 10^5$) were inoculated into the right flank of WT mice at 6 weeks of age. Six days after subcutaneous inoculation, the mice were randomly divided into different groups. *P. gingivalis* ($10^6$ CFU) was given by multipoint intratumoral injection twice per week for three weeks. The mice were euthanized before the tumors were dissected.

### Bone marrow chimera generation

Recipient WT mice were lethally irradiated with a total dose of 12 Gy, followed by bone marrow (BM) reconstitution with cells from the femurs and tibiae of *NLRP3*$^{-/-}$ or control mice. After allowing 8 weeks for reconstitution, the mice were bled, and qPCR was performed to examine the rate of reconstitution. The mice were then ready for use in orthotopic colorectal xenograft experiments.

### IHC staining

We employed IHC staining to detect the existence of *P. gingivalis* since several investigations have shown that IHC staining with *P. gingivalis*–specific antibodies has the highest sensitivity and specificity and produces relatively good interobserver agreement (19). Tissue sections were deparaffinized and rehydrated prior to antigen retrieval in citrate buffer. The sections were then stained with a monoclonal mouse anti-RgpB antibody (1:100; gift from the laboratory of Jin-Long Gao, University of Sydney, New South Wales, Australia) for the detection of *P. gingivalis*. Positive and negative control sections were always included in the IHC staining protocol.

### FISH

FISH was carried out with appropriate specific probes according to the manufacturer's instructions. Tissue sections were probed with 5 mg/mL *P. gingivalis* 16S rRNA-specific oligonucleotide POGI 5'-CAATACTC GTATCGCCCGTTATTC-3' labeled with Cy3 dye (Takara, Japan). Images were analyzed using a fluorescence microscope.

### Pathology assessment

Each IHC staining result was confirmed by a tissue slide from the same patient. The slides were scanned by Zeiss Axioplan 2 imaging E for digital image analysis. The images were blindly reviewed and scored by two certified anatomic pathologists. *P. gingivalis* staining was defined as cytoplasmic DAB staining (sepia areas as shown in **Fig. 1D**). Staining percentages refer to the rate of positive cells among all cells in one 400× field. The staining intensity was classified using a numerical scale: grade 0 (negative, 0%–10% staining); grade 1 (weak, 10%–30%); grade 2 (moderate, 30%–60%); and grade 3 (strong, over 60%) as described previously (19); however, the total number of high (60%+) groups in our previous study was zero. Therefore, we can only simplify the original criteria by dividing the percentages into three groups: negative (0%–10%), weak (10%–30%), and strong (30%+). Then, the three grades were categorized into low (negative and weak) and high (strong) expression for statistical analysis.

### DNA extraction and qPCR

DNA was extracted from all fecal samples with E.Z.N.A. Stool DNA Kit (Omega Biotek), and biopsies were extracted with an AllPrep DNA/RNA Mini Kit (Qiagen, Hilden, Germany). A NanoDrop 2000 Spectrophotometer (Thermo Fisher Scientific) was used to measure the concentration and purity of the extracted DNA. DNA from biopsy and stool samples was diluted 10- and 100-fold, respectively, in PCR-grade water to facilitate downstream analysis. Relative abundance was calculated by the $\Delta C_t$ method. Quantitative real-time PCR was performed in triplicate with an Applied LightCycler 96 quantitative PCR system (Roche). In human tissue samples, the cycle threshold ($C_t$) values for *P. gingivalis* were normalized to the amount of human biopsy DNA in each reaction by using a primer/probe set for the reference gene, prostaglandin transporter (PGT), as previously described (20). In human stool samples and mouse samples, the $C_t$ values for *P. gingivalis* were normalized using a primer/probe set for the total bacteria. The primer and probe sequences for each assay were as follows: *P. gingivalis* forward primer, 5′-TGCAAACCCATCACC-TTCAAGAC-3′; *P. gingivalis* reverse primer, 5′-TCCTTGCTTCTCT-TCCTCGGT-3′; *P. gingivalis* FAM probe: TGCACAAGGCACAA-CGCAACAGGGCA; PGT forward primer, 5′-ATCCCCAAAG-CACCTGGTTT-3′; PGT reverse primer, 5′-AGAGGCCAAGATAG-TCCTGGTAA-3′; PGT FAM probe, 5′-CCATCCATGTCCTCAT-CTC-3′; Eubacteria 16S forward primer, 5′-GGTGAATACGTTCC-CGG-3′; Eubacteria 16S reverse primer, 5′- TACGGCTACCTTGT-TACGACTT-3′.

### RNA sequencing and analysis

High-throughput sequencing was performed by CapitalBio Technology (CapitalBio Technology Inc.). Each sample was cleaned up on an RNeasy MinElute spin column (QIAGEN), double-stranded DNA was generated by the NEBNext Ultra Directional RNA Second Strand Module (NEBNEXT, New England Biolabs, Inc.) and then analyzed for quality on an Agilent 2100 Bioanalyzer. Samples were run on an Illumina HiSeq 3000 for 2 × 150-bp paired-end sequencing. Reads were aligned to the mouse genome (Ensembl release 82-GRCm38) using TopHat and default parameters. To calculate transcript abundances, we used Cufflinks v2.2.1 to convert raw reads to FPKM values. Analysis was performed using the Ingenuity Pathway Analysis (IPA) database (21) and the Kyoto Encyclopedia of Genes and Genomes (KEGG) database (22) considering genes differentially expressed between the *P. gingivalis* group and the BHI broth group, with adjusted $P < 0.05$ and absolute fold change > 2.

### 16S rRNA amplicon sequencing and analysis

16S rRNA sequencing was performed by the Microbial Genome Research Center (IMCAS, Beijing, China). Briefly, DNA of the stool sample was extracted as stated above, and the V3 and V4 regions of the bacterial 16S rDNA gene were amplified. Purified amplicons were pooled in equimolar amounts and paired-end sequenced (2 × 250) on an Illumina MiSeq platform according to standard protocols. The raw reads were deposited into the NCBI Sequence Read Archive (SRA) database. Fast Length Adjustment of SHort reads (FLASH) was used to merge paired-end reads from next-generation sequencing (23). Low-quality reads were filtered by fastq_quality_filter (-p 90 -q 25 -Q33) in FASTX Toolkit 0.0.14, and chimera reads were removed by USEARCH 64 bit v8.0.1517. The number of reads for each sample was normalized based on the smallest size of samples by random

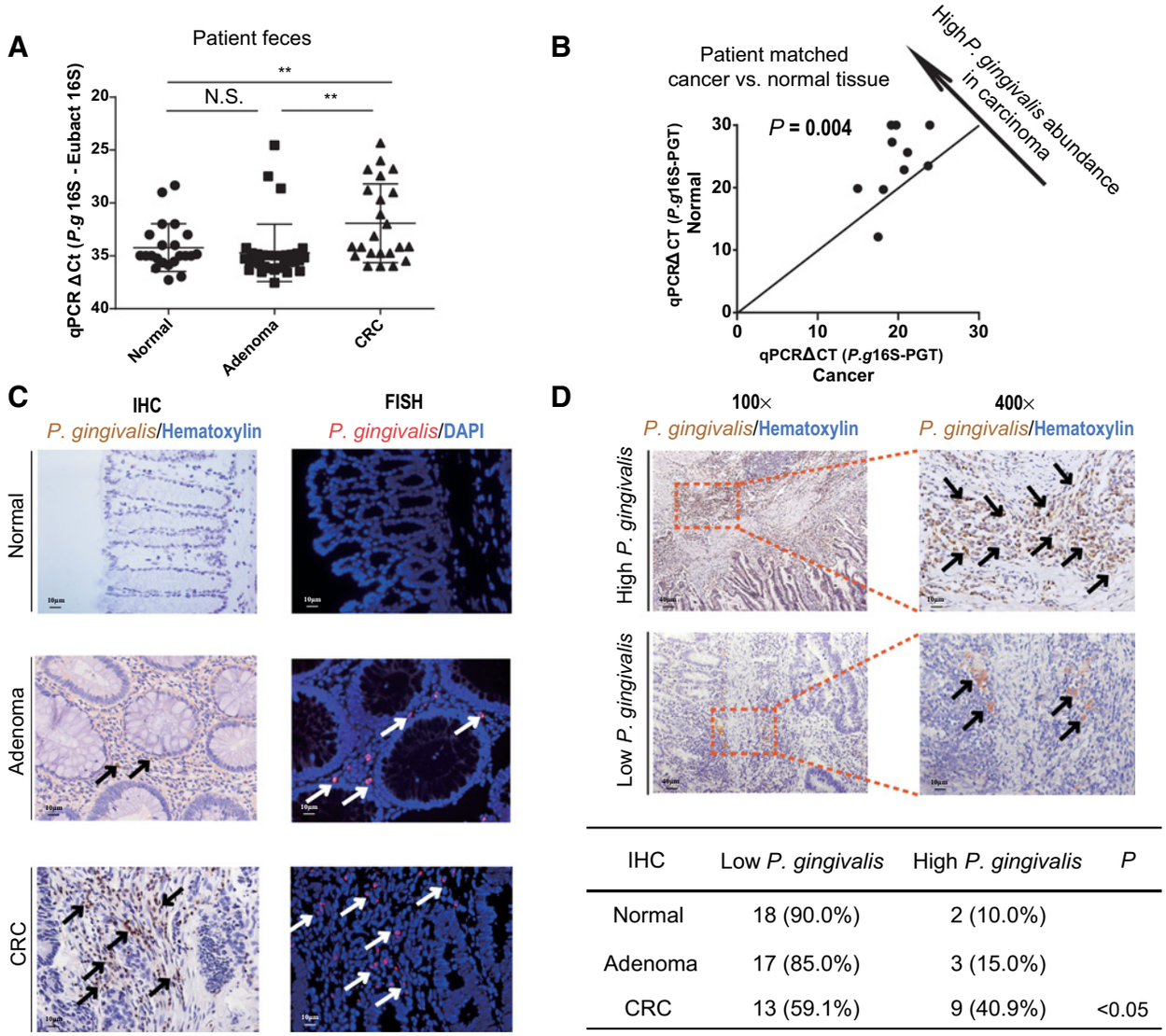


| IHC | Low *P. gingivalis* | High *P. gingivalis* | *P* |
|---|---|---|---|
| Normal | 18 (90.0%) | 2 (10.0%) | |
| Adenoma | 17 (85.0%) | 3 (15.0%) | |
| CRC | 13 (59.1%) | 9 (40.9%) | <0.05 |

**Figure 1.**

*P. gingivalis* was detected at a higher abundance in stool and tissues from colorectal cancer patients than in those from patients with adenoma and healthy controls and was enriched in carcinoma tissue versus adjacent normal tissue. **A,** Fecal abundance of *P. gingivalis* was assessed in samples from normal controls ($n = 22$), subjects with colorectal adenoma ($n = 32$), and subjects with colorectal cancer ($n = 23$) using TaqMan probe-based qPCR. **B,** The *P. gingivalis* abundance in carcinoma (*x*-axis) versus that in paired normal tissue (*y*-axis) is plotted. The $C_t$ values for *P. gingivalis* were normalized to the reference gene PGT. qPCR ΔCt (P.g 16S-PGT) represents the relative $C_t$ value of *P. gingivalis* and PGT. **C,** Representative IHC and FISH images of *P. gingivalis* in normal controls, human adenoma, and human colorectal cancer (CRC) samples using monoclonal mouse anti-RgpB antibody or a Cy3-conjugated *P. gingivalis* 16S rDNA-directed probe (red; arrows, *P. gingivalis* colonization, 400×). **D,** Representative IHC-stained paraffin sections of high and low staining of *P. gingivalis* using monoclonal mouse anti-RgpB antibody in human colorectal cancer samples (arrows, *P. gingivalis* colonization, 400×). The percentage of low and high *P. gingivalis* infection in normal controls, human adenoma, and human colorectal cancer samples is shown (the mean percentage ± SEM is shown; **, $P < 0.01$ by Student *t* test; N.S., not significant).

subtraction. OTUs were aligned by the UCLUST algorithm with 97% identity and taxonomically classified using the SILVA 16S rRNA database v128. We used the linear discriminant analysis (LDA) effect size (LEfSe) method to identify species that showed statistically significant differential abundances among groups (24).

### Isolation of tumor-infiltrating cells

Tumors were dissected and homogenized using a Gentle MACS dissociator (Miltenyi Biotec) and digested with 0.05% collagenase IV (Sigma-Aldrich) and 0.002% DNase I (Roche) at 37°C for 1 hour prior to resuspension in RPMI.

### Flow cytometry

Single-cell preparation was incubated with Fc blocking antibody (BioLegend), stained for dead cells using a Zombie NIR Fixable Viability Kit (BioLegend) and mAbs of cell surface markers. For intracellular staining, cells were stimulated with 50 ng/mL PMA (Sigma-Aldrich) and 5 μg/mL ionomycin (Sigma-Aldrich) in the

presence of brefeldin A (BioLegend), followed by dead cell and surface marker staining and fixation prior to intracellular staining for cytokines. The following antibodies were used for flow cytometry: anti-mouse CD45 (clone 30-F10), anti-mouse Gr-1 (clone 1A8 LY6G); anti-mouse Ly-6G (clone RB6–8C5); anti-mouse Ly-6C (clone HK1.4); anti-mouse CD11b (clone M1/70); anti-mouse CD11c (clone N418); anti-mouse MHC II (clone MS/114.15.2); anti-mouse F4/80 (clone BM8); anti-mouse CD3 (clone KT3); anti-mouse CD4 (clone RM4–5); anti-mouse CD8 (clone 3B5); anti-mouse IFNγ (clone B27); and anti-mouse CD56 (clone MEM-188). The number of isolated live single cells from tumor tissues was measured as the cell number/gram of tumor tissue. In flow cytometric analysis, the percentage of live $CD45^+$cells among the total singlet cells was first determined. Each immune cell subset was identified by specific lineage markers. The gating strategy for each immune cell subset is presented in **Fig. 5** and Supplementary Fig. S1. The number of cells in each immune cell subset was calculated as the cell number/gram of tumor tissue by multiplying the percentage.

### ELISA

THP1 cells obtained from ATCC in 2016 were tested for authentication and *Mycoplasma* contamination within 6 months. THP-1 cells used were no more than 15 passages. THP-1 cells ($2 \times 10^6$ cells/well) were treated with *P. gingivalis* [multiplicity of infection (MOI) = 100] for 3, 6, 12, and 24 hours at 37°C in a 5% $CO_2$ humidified atmosphere prior to the assay. The tumors from the *P. gingivalis* group and control group were processed into single-cell suspensions that were cultured for 48 hours. The cell supernatant was collected, and the levels of the cytokines IL1β, IL6, and TNFα were determined by using ELISA kits according to the manufacturer's protocols (Mlbio, Inc.).

### Statistical analysis

Statistical analyses were carried out using PASW Statistics 18 (SPSS Inc.) and GraphPad Prism 6 (GraphPad Software, Inc.). The difference in measurement data between two groups was assessed using a nonparametric Mann–Whitney test for nonnormal descriptive data and a *t* test for normal descriptive data. Categorical data were analyzed with the $\chi^2$ test or Fisher exact test. Kaplan–Meier survival analyses were performed for the two cohorts. Cox regression was performed for the univariate and multivariate regression analyses. Variates with statistical significance ($P < 0.05$) in univariable Cox regression model analysis were chosen to adjust covariates in the multivariable regression models.

## Results

### *P. gingivalis* is enriched in samples from patients with colorectal cancer

Given that *Porphyromonas* is enriched in feces from patients with colorectal cancer compared with feces from controls (10), we first examined whether *P. gingivalis* was enriched in fecal samples from 77 subjects. The participants included 22 control subjects with no prior history of colorectal cancer or gastrointestinal disease, which was confirmed by bowel preparation and colonoscopy screening; 32 subjects with colorectal adenoma; and 23 subjects with colorectal cancer. We compared the levels of *P. gingivalis* in the feces from the individuals in each group by TaqMan probe–based quantitative real-time (qPCR) analysis and observed an increased abundance of *P. gingivalis* in the colorectal cancer group compared with the adenoma and healthy donor groups ($P < 0.01$, **Fig. 1A**). These results indicate that the trend toward an increased abundance of *P. gingivalis* in the gut microbiota may be a general feature of colorectal cancer.

Then, we examined whether *P. gingivalis* colonized colorectal cancer tissue by TaqMan qPCR, IHC staining with an anti-Rgp antibody and FISH with a *P. gingivalis* 16S rDNA-directed probe (POGI). We found that *P. gingivalis* could be detected by qPCR in 10 samples among 31 colorectal cancer samples with paired normal tissues. In the positive samples, *P. gingivalis* was enriched in colorectal cancer tissue relative to paired normal tissue (paired *t* test, $P = 0.004$; **Fig. 1B**). Further IHC and FISH staining confirmed that *P. gingivalis* was detected in the FFPE colorectal cancer, adenoma, and normal tissue samples (**Fig. 1C**). The IHC staining intensity for *P. gingivalis* abundance was initially classified as negative, weak, and strong according to the positive cell rate (negative, 0%–10%; weak, 10%–30%; strong, over 30%) and then categorized into low (less than 30%) and high (over 30%) expression groups. The high levels of *P. gingivalis* in the colorectal cancer group (40.9%) was significantly higher than that in the adenoma and normal groups ($\chi^2$ test, $P < 0.05$; **Fig. 1D**). Consequently, our results showed that *P. gingivalis* accumulated during advanced stages of colonic tumorigenesis in patients with colorectal cancer.

### *P. gingivalis* is associated with colorectal cancer recurrence and patient survival

We next evaluated the relationship between *P. gingivalis* abundance and patient outcomes in FFPE samples from patients with colorectal cancer in two cohorts. The baseline characteristics, including sex, age, smoking status, and alcohol consumption, between the high and low *P. gingivalis* infection groups was not significantly different in the two cohorts ($\chi^2$ test, $P > 0.05$; Supplementary Tables S1 and S2). We used IHC staining to detect the presence of *P. gingivalis* in FFPE samples derived from clinical colorectal cancer specimens. When we analyzed the associations of staining intensity with patient outcome, we categorized the IHC staining intensity as low (positive cell rate less than 30%) and high (positive cell rate over 30%) expression (**Fig. 1D**).

The staging of colorectal cancer is an important prognostic indicator (25). In both cohorts, T stage and N stage were positively associated with poor overall survival (OS) and shorter 5-year recurrence-free survival (RFS). *P. gingivalis* abundance and its prognostic value were then examined. Cohort 1 contained 155 samples from the Sixth Affiliated Hospital of Sun Yat-sen University in southern China; 44 samples (28.4%) had tumors that exhibited a high overall *P. gingivalis* abundance. Abnormally high *P. gingivalis* abundance was positively associated with poor OS [HR = 6.07; 95% confidence interval (CI), 4.22–22.13; $P < 0.001$ by the log-rank test; **Fig. 2A**] and shorter 5-year RFS (HR = 6.48; 95% CI, 4.71–24.21; $P < 0.001$ by the log-rank test; **Fig. 2B**). In addition, univariate (Supplementary Table S3) and multivariate (Supplementary Table S4) Cox regression analyses of cohort 1 demonstrated that the amount of *P. gingivalis* was an independent predictor of colorectal cancer aggressiveness with significant HRs for predicting clinical outcomes (OS: HR = 2.36; 95% CI, 1.02–5.48, multivariate Cox regression, $P = 0.046$; RFS: HR = 2.98; 95% CI, 1.32–6.72, multivariate Cox regression, $P = 0.008$; **Fig. 2C**).

Cohort 2 comprised 237 FFPE colorectal cancer samples from the Affiliated Hospital of Inner Mongolia Medical University in the northern region of China; of these, 76 (32.07%) had tumors that exhibited a high overall *P. gingivalis* abundance. High levels of *P. gingivalis* were positively associated with poor OS (HR = 2.31; 95% CI, 1.69–4.19, $P < 0.001$ by the log-rank test; **Fig. 2D**) and shorter 5-year RFS (HR = 2.15; 95% CI, 1.59–4.13, $P < 0.001$ by the log-rank

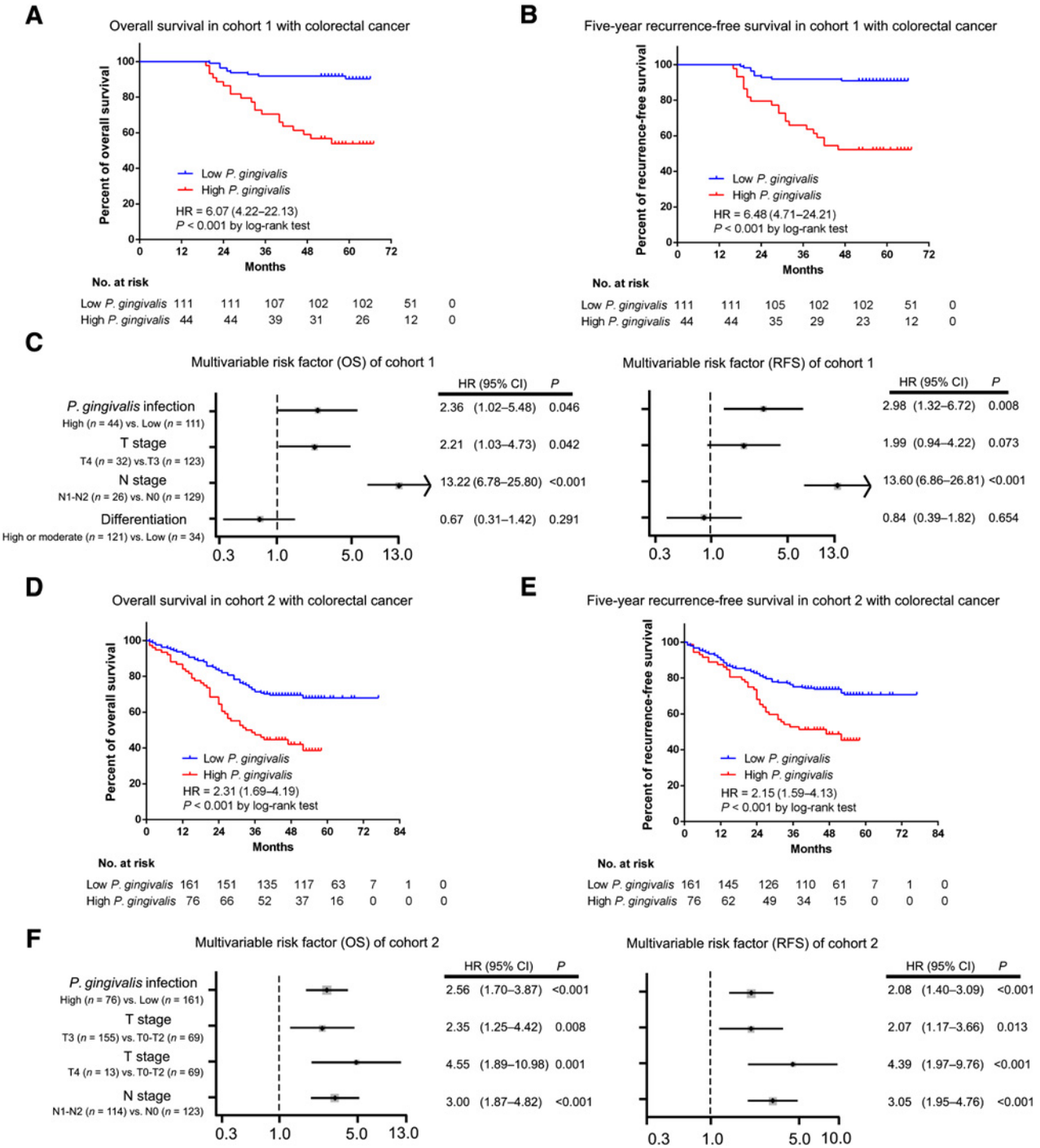


**Figure 2.**

*P. gingivalis* is associated with cancer recurrence and patient outcomes. **A,** OS was compared between patients in cohort 1 with a low abundance of *P. gingivalis* and those with a high abundance of *P. gingivalis* by using the log-rank test. **B,** RFS was compared between patients in cohort 1 with a low abundance of *P. gingivalis* and those with a high abundance of *P. gingivalis* by using the log-rank test. **C,** Adjusted multivariable risk factor cohort of OS and RFS in cohort 1. A high abundance of *P. gingivalis* was significantly associated with short OS and poor RFS. **D,** OS was compared between the patients in cohort 2 with a low abundance of *P. gingivalis* and those with a high abundance of *P. gingivalis* by using the log-rank test. **E,** RFS was compared between the patients in cohort 2 with a low abundance of *P. gingivalis* and those with a high abundance of *P. gingivalis* by using the log-rank test. **F,** Adjusted multivariable risk factor cohort of OS and RFS in cohort 2. A high abundance of *P. gingivalis* was significantly associated with short OS and poor RFS.

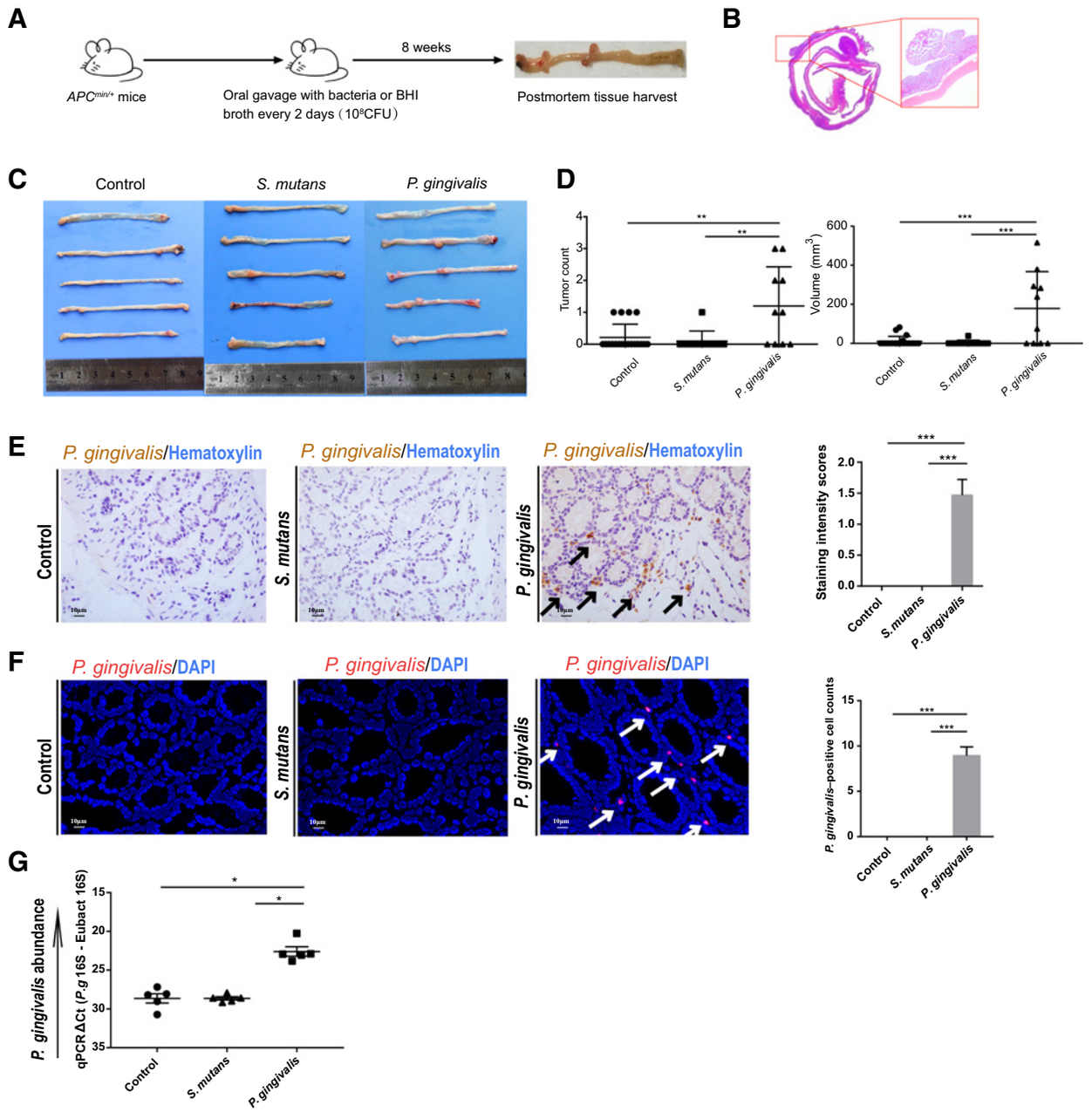


**Figure 3.**

*P. gingivalis* promotes tumorigenesis in Apc$^{Min/+}$ mice. **A,** Schematic diagram showing the experimental protocol used to determine the role of *P. gingivalis* in promoting colorectal tumorigenesis in Apc$^{Min/+}$ mice. Apc$^{Min/+}$ mice were gavaged with *P. gingivalis* ($n = 10$), *S. mutans* ($n = 10$), or BHI broth ($n = 20$) for 8 weeks before undergoing euthanasia. **B,** A representative hematoxylin and eosin–stained image is shown. The frame indicated adenomas in the left image. Representative *in situ* images of colons (**C**) and the tumor count and volume in the colons (**D**). The group gavaged with *P. gingivalis* showed higher tumor counts and larger tumor volumes than the *S. mutans* and control groups. **E,** Representative IHC-stained paraffin sections of the tumor tissue from Apc$^{Min/+}$ mice gavaged with *P. gingivalis, S. mutans*, or BHI broth (arrows, *P. gingivalis* infection, 400×). The intensity scores of *P. gingivalis* infection are shown. **F,** Representative FISH image of tumor tissue from Apc$^{Min/+}$ mice gavaged with *P. gingivalis, S. mutans*, or BHI broth using a Cy3-conjugated *P. gingivalis* 16S rDNA–directed probe (red; arrows, *P. gingivalis* infection, 400×). The number of cells positive for *P. gingivalis* infection per 400× field is shown. **G,** The abundance of *P. gingivalis* was determined in colon tumor tissues from the three groups using TaqMan probe-based quantitative qPCR. The mean percentage ± SEM is shown. *, $P < 0.05$; **, $P < 0.01$; ***, $P < 0.001$ by Student *t* test.

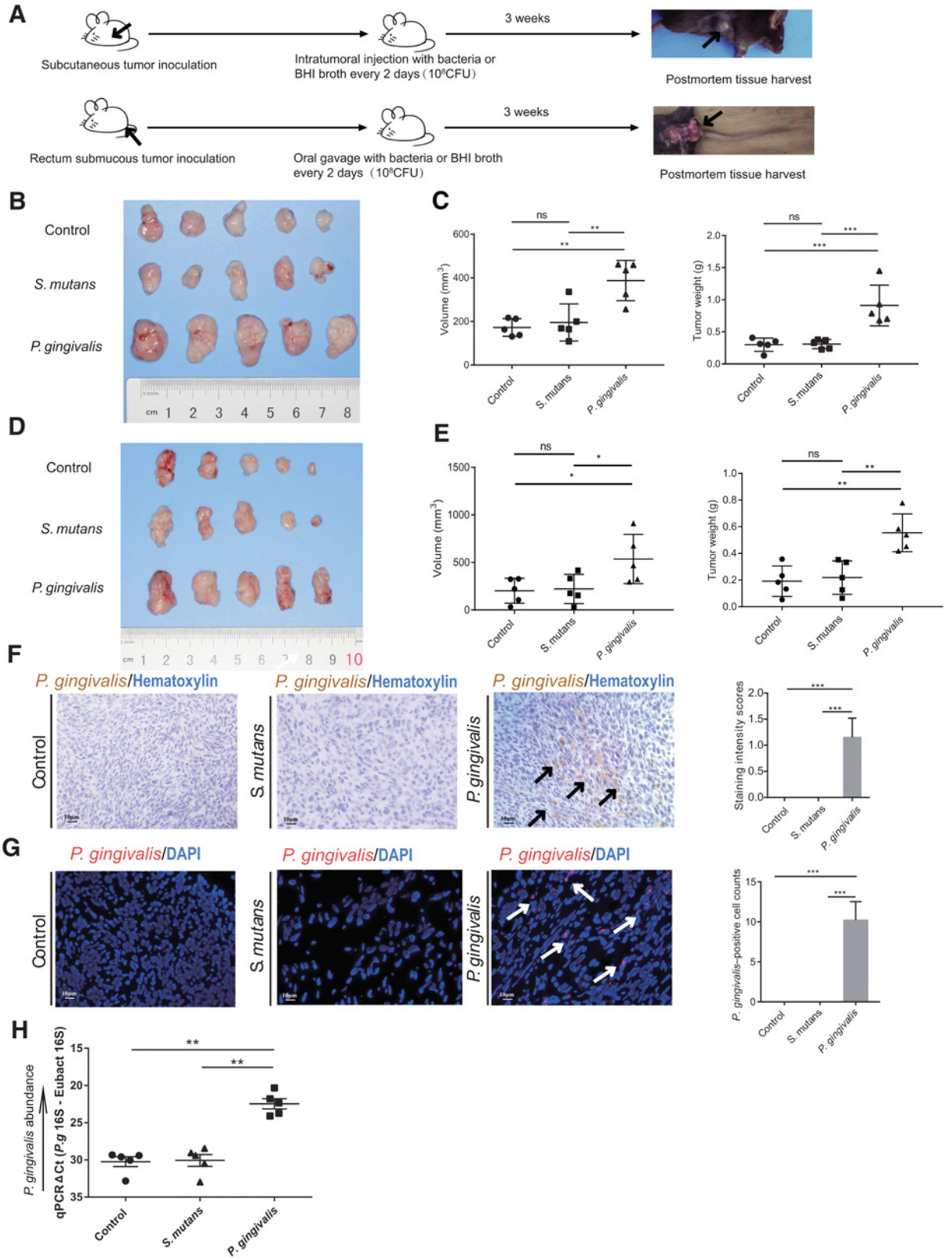

test; **Fig. 2E**). In addition, univariate (Supplementary Table S5) and multivariate (Supplementary Table S6) regression analyses of cohort 2 confirmed that the amount of *P. gingivalis* was an independent predictor of colorectal cancer aggressiveness with significant HRs for predicting clinical outcomes (OS: HR = 2.56; 95% CI, 1.70–3.87, multivariate Cox regression, $P < 0.001$; RFS: HR = 2.08, 95% CI, 1.40–3.09, multivariate Cox regression, $P < 0.001$; **Fig. 2F**). Thus, the data in cohort 1 and cohort 2 confirmed the potential value of the presence of *P. gingivalis* in predicting colorectal cancer recurrence and patient outcomes.

### *P. gingivalis* promotes colorectal tumorigenesis

The enrichment of *P. gingivalis* in colorectal cancer prompted us to confirm whether *P. gingivalis* contributes to the initiation and progression of tumors in mouse models. We utilized a model mouse that develops intestinal tumors because of a mutation in one copy of the tumor suppressor gene *Apc* (C57BL/6 $Apc^{Min/+}$ mice). $Apc^{min/+}$ mice are widely used to simulate the tumorigenesis of colorectal tumors (26). We administered *P. gingivalis* ATCC 33277 (*P. gingivalis* group), *Streptococcus mutans* UA159 (*S.m* group), or brain-heart infusion (BHI) broth (control group) to $Apc^{Min/+}$ mice via oral gavage (**Fig. 3A**). *S. mutans* UA159 was used as a negative control because *Streptococcus* spp. has been shown to lack an obvious effect on colorectal adenoma in this model (5). The mice were gavaged with bacteria or BHI broth twice a week from 6 weeks old to 14 weeks old, and the development of intestinal tumors was monitored (**Fig. 3B**). The introduction of *P. gingivalis* into $Apc^{Min/+}$ mice increased the onset of colonic tumors (**Fig. 3C**), with these mice presenting a significantly higher multiplicity ($P < 0.01$; **Fig. 3D**) of colonic tumors and larger total colonic tumor volume ($P < 0.001$; **Fig. 3D**) compared with those in $Apc^{Min/+}$ mice gavaged with BHI broth or *S. mutans*. *P. gingivalis* was enriched in the tumor tissue of the *P. gingivalis*–gavaged $Apc^{Min/+}$ mice, as indicated by IHC ($P < 0.001$; **Fig. 3E**) and FISH assays ($P < 0.001$; **Fig. 3F**). We compared the levels of *P. gingivalis* by quantitative qPCR and found that the abundance of *P. gingivalis* in tumor tissues collected from the *P. gingivalis* group was significantly higher than that in tumor tissues collected from the control or *S. mutans* groups ($P < 0.05$; **Fig. 3G**). These data suggested that *P. gingivalis* colonization of colorectal adenoma could promote colorectal tumorigenesis.

### *P. gingivalis* promotes colorectal tumor progression in a colorectal cancer xenograft mouse model

We next explored whether *P. gingivalis* can enhance colorectal tumor progression. Subcutaneous and orthotopic MC38 rectal carcinoma models have been widely used to study colorectal tumor growth (6, 27). The two models were used to determine whether *P. gingivalis* can colonize colorectal cancer tissue and promote tumor progression (**Fig. 4A**). Mice with subcutaneous colorectal cancer were intratumorally injected with *P. gingivalis, S. mutans*, or BHI broth, and the tumor tissue was harvested 3 weeks later. The introduction of *P. gingivalis* into the subcutaneous xenografts in mice increased tumor weight and volume ($P < 0.01$, $P < 0.001$; **Fig. 4B** and **C**). In another colorectal cancer xenograft mouse model, MC38 cells were injected through the rectum into the submucosa, and *P. gingivalis* was administered by oral gavage. As in the subcutaneous model, *P. gingivalis* increased the tumor weight and volume in this orthotopic model ($P < 0.05$, $P < 0.01$; **Fig. 4D** and **E**). *P. gingivalis* was enriched in the tumor tissue of *P. gingivalis*–gavaged mice, as assayed by IHC and FISH ($P < 0.001$; **Fig. 4F** and **G**). In addition, the enrichment of *P. gingivalis* in tumor tissues was confirmed by qPCR ($P < 0.01$; **Fig. 4H**). To characterize the impact of *P. gingivalis* on the resident microbiome in the colon, we performed 16S rRNA gene sequencing on the feces from orthotopic mice. Verrucomicrobiaceae was the most abundant family and was prevalent in all samples (Supplementary Fig. S1A). Erysipelotrichaceae, which is known to be associated with inflammation-related disorders of the gastrointestinal tract and was found to be increased in the lumen of patients with colorectal cancer compared with healthy controls (28), showed the largest increase in the *P. gingivalis* group compared with the BHI group. Moreover, the bacterial composition in the *P. gingivalis* group was distinct from that of the control group based on the assessment of clade abundances using linear discriminant analysis effect size (LEfSe; Supplementary Fig. S1B). These data indicated that *P. gingivalis* can change the mouse gut microbiome and increase tumor growth in xenograft mouse models.

### *P. gingivalis* changes the tumor immune environment by selectively expanding myeloid-derived immune cells and inducing a proinflammatory microenvironment

To address whether *P. gingivalis* contributes to tumorigenesis by affecting intratumoral immune cells and the inflammatory microenvironment, we first characterized tumor-infiltrating immune cells from orthotopic MC38 rectal carcinomas in mice gavaged with *P. gingivalis* ATCC 33277 or BHI broth. We observed an increase in the accumulation of infiltrating myeloid lineage cells. The numbers of $CD11b^+$ myeloid cells, $CD11b^+$ MHC class $II^+$ myeloid antigen-presenting cells, and differentiated myeloid cells, such as macrophages and dendritic cells (DC), were increased in orthotopic MC38 rectal carcinomas from mice gavaged with *P. gingivalis* compared with those from the control mice ($P < 0.05$; **Fig. 5A** and **B**). The effect of *P. gingivalis* on other tumor-infiltrating immune cells was also explored. The numbers of $CD3^+CD4^+$ T cells, $CD3^+CD8^+$ T cells, and natural killer (NK) cells were not significantly different between the two groups (Supplementary Fig. S2A and S2B). IFNγ secretion from $CD3^+CD4^+$ T cells and $CD3^+CD8^+$ T cells was also not diminished (Supplementary Fig. S2C). To further confirm the changes in the immune microenvironment induced by *P. gingivalis*, we

**Figure 4.**

*P. gingivalis* promotes colorectal cancer tumor growth in a xenograft mouse model. **A,** Schematic diagram showing the experimental protocol used to determine the role of *P. gingivalis* in promoting colorectal tumor growth in C57BL/6 mice. Two xenograft mouse models were used. Mice were administered *P. gingivalis* via intratumoral injection in the subcutaneous MC38 tumor model or via oral gavage in the colon submucosal MC38 tumor model at 6 weeks of age; control mice were injected or orally gavaged with *S. mutans* or BHI broth. **B,** Representative *in situ* image ($n = 5$) of MC38 tumors from subcutaneous MC38 tumor model mice intratumorally injected with *P. gingivalis, S. mutans*, or BHI broth. **C,** The tumor volume and weight are shown. Tumor volume was measured and calculated using the following formula: $V = L \times W^2/2$. **D** and **E,** Representative *in situ* image of MC38 tumors from colon submucosal MC38 tumor model mice subjected to oral gavage of *P. gingivalis, S. mutans*, or BHI broth. The tumor volume and weight of each group are shown. **F** and **G,** IHC and FISH analyses of paraffin tissue sections of tumor tissue harvested from mice subjected to oral gavage with *P. gingivalis, S. mutans*, or BHI broth (arrows, *P. gingivalis* infection, 400×). **H,** TaqMan probe-based qPCR was used to determine the abundance of *P. gingivalis* in tumor tissues harvested from mice subjected to oral gavage with *P. gingivalis, S. mutans*, or BHI broth. The mean percentage ± SEM is shown. *, $P < 0.05$; **, $P < 0.01$; ***, $P < 0.001$ by Student *t* test; ns, not significant; one representative experiment of two replicates is shown.

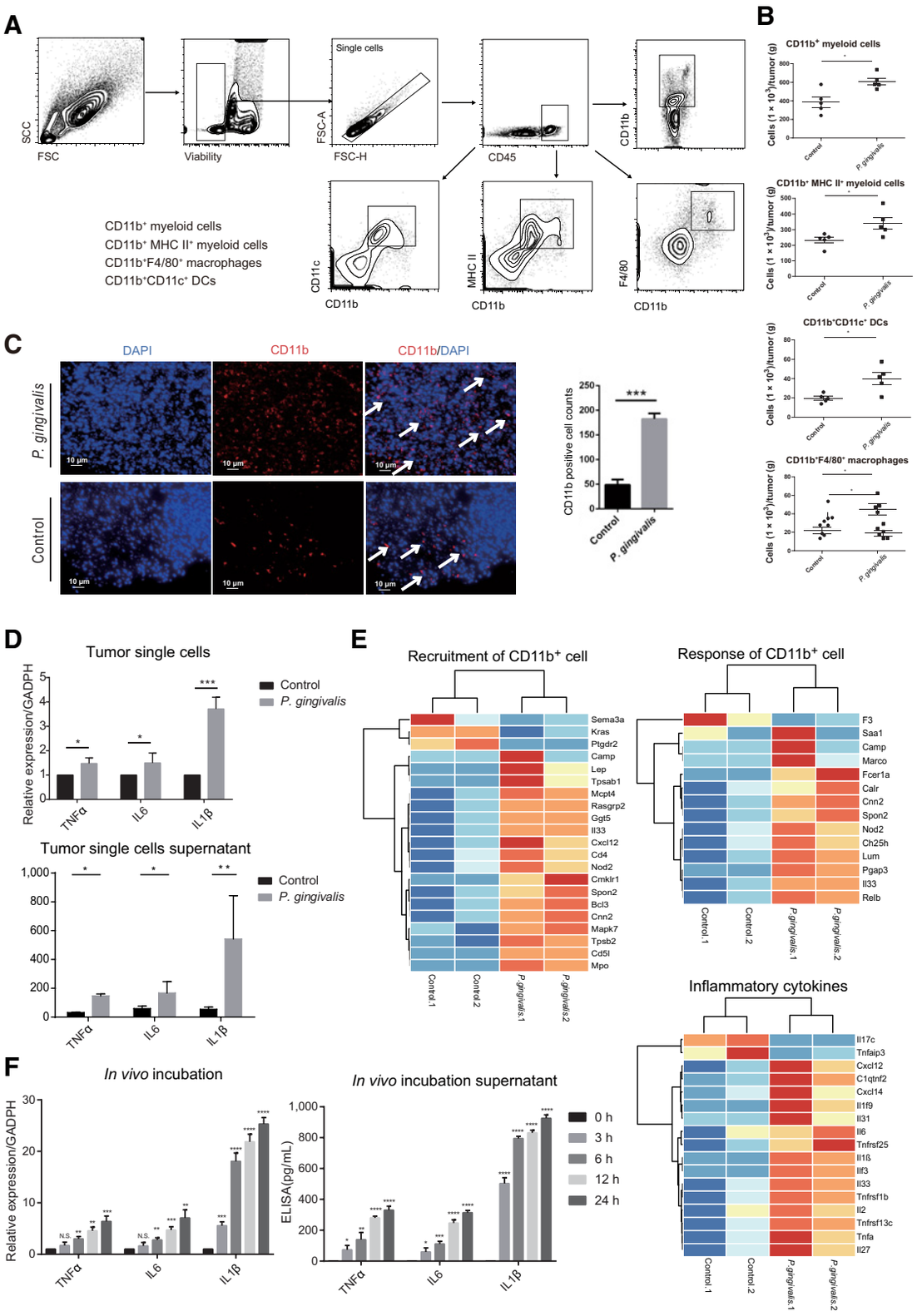

compared CD11b$^+$ myeloid cell infiltration in FFPE samples from the *P. gingivalis* group and control group by IHC staining (anti-CD11b antibodies). The samples from the *P. gingivalis* group (which had higher accumulation of *P. gingivalis*) were shown to have higher accumulation of CD11b$^+$ myeloid cells ($P < 0.001$; **Fig. 5C**). To further explore the inflammatory microenvironment of tumors from mice gavaged with *P. gingivalis*, the levels of proinflammatory cytokines such as TNFα, IL6, and IL1β were measured. The results showed increased levels of TNFα, IL6, and IL1β in the *P. gingivalis* group ($P < 0.05$, $P < 0.05$, $P < 0.001$; **Fig. 5D**). Interestingly, the secretion of IL1β was 3-fold higher than that of TNFα and IL6 ($P < 0.001$; **Fig. 5D**).

We also performed transcriptome sequencing of tumors from the orthotopic rectal carcinoma mouse model. Differentially expressed genes were analyzed by using IPA and KEGG database, and these analyses confirmed that compared with mice in the BHI group, mice in the *P. gingivalis* group presented a tumor immune microenvironment enriched in myeloid cells and inflammatory cytokines, which corresponds to a proinflammatory tumor microenvironment (**Fig. 5E**).

Because the above results indicated myeloid cell enrichment and a proinflammatory microenvironment, we further investigated whether *P. gingivalis* can directly activate myeloid cells. The myeloid cell line THP1 was infected with *P. gingivalis* for 3, 6, 12, and 24 hours (MOI = 100) *in vitro*. We extracted total RNA and collected the supernatants of these samples after the infection period and measured TNFα, IL6, and IL1β levels by qPCR and corresponding ELISAs; *P. gingivalis* increased the levels and secretion of TNFα, IL6, and IL1β by THP1 cells (**Fig. 5F**). The above results suggested that *P. gingivalis* is a potential initiator of colorectal cancer that alters the immune microenvironment of tumors by recruiting myeloid cells and induces myeloid cells to release proinflammatory cytokines such as TNFα, IL6, and IL1β. Taken together, the above results show that *P. gingivalis* alters the tumor immune microenvironment by selectively expanding myeloid-derived immune cells and promoting a proinflammatory microenvironment.

### *P. gingivalis* can activate the NLRP3 inflammasome *in vitro* and fails to induce colorectal tumor growth in *NLRP3*$^{-/-}$ mice

We have demonstrated that *P. gingivalis* activates the production and secretion of IL1β in tumor tissues and cultured cells. The activation of IL1β is regulated by two processes: the transcription of pro-IL1β mRNA regulated by nuclear factor (NF)-κB and the maturation of IL1β regulated by the inflammasome complex. Several different inflammasomes have been discovered, of which the NLRP3 inflammasome is the most intensively studied. To assess the role of the NLRP3 inflammasome in the *P. gingivalis*–induced secretion of IL1β, the expression of the NLRP3 inflammasome in CD45$^+$ immune cells derived from tumor lysates of a submucosal MC38 tumor model was detected by qPCR. The results showed that the NLRP3 inflammasome level was elevated in the tumor-infiltrating immune cells from the *P. gingivalis* group ($P < 0.001$; **Fig. 6A**). Because *P. gingivalis* selectively recruits myeloid cells and induces a proinflammatory microenvironment in colorectal cancer, BM–derived macrophages (BMDM), which are the primary macrophage lineage derived from myeloid progenitors, were chosen for the *in vitro* study. After BMDMs were cocultured with *P. gingivalis* for 4 or 8 hours, they were processed for immunoblotting detection of NLRP3, pro-IL1β and procaspase-1 expression, while cell culture supernatants were evaluated for IL1β and caspase-1 levels. We found that *P. gingivalis* could induce NLRP3, caspase-1, IL1β and pro-IL1β expression in a time-dependent manner, but no change in procaspase-1 levels was observed in these cells (**Fig. 6B** and **C**). The role of NLRP3 in the *P. gingivalis*–induced secretion of IL1β was further determined in C57BL/6 WT mice and *NLRP3*$^{-/-}$ mice by using the same BMDM coculture model. We found that NLRP3 knockdown significantly inhibited *P. gingivalis*–induced caspase-1 activation and subsequent IL1β secretion but did not affect the levels of procaspase-1 (**Fig. 6D**).

Next, we explored whether *P. gingivalis* promotes colorectal cancer via *NLRP3* activation *in vivo*. Strikingly, the colorectal cancer tumor weight and volume in the *P. gingivalis* group were significantly decreased in *NLRP3*$^{-/-}$ mice compared with WT mice (**Fig. 6E**). Flow cytometry analysis of tumor tissues from *NLRP3*$^{+/+}$ mice showed myeloid cell enrichment in the *P. gingivalis* group, whereas *NLRP3*$^{-/-}$ mice showed no myeloid cell enrichment ($P < 0.05$, $P < 0.01$; **Fig. 6F**).

### Hematopoietic *NLRP3* is required for *P. gingivalis*–induced colorectal cancer development

NLRP3 is mainly expressed in cells of the myeloid lineage but is also expressed in epithelial cells. To determine the cell populations that are critical for NLRP3-dependent tumorigenesis, we generated irradiated BM chimeric mice that selectively express NLRP3 in specific cellular compartments (i.e., in hematopoietic or somatic cells) and infected them with *P. gingivalis* (**Fig. 7A**). In line with our previous observations, NLRP3 expression in the hematopoietic compartment (NLRP3$^{+/+}$ → NLRP3$^{+/+}$) enhanced colorectal cancer tumor weight and volume compared to that in the NLRP3-deficient hematopoietic compartment (NLRP3$^{-/-}$ → NLRP3$^{+/+}$; **Fig. 7B**). An identical disease pattern was observed for myeloid cell recruitment: mice with selective deletion of NLRP3 in the hematopoietic compartment (NLRP3$^{-/-}$ →NLRP3$^{+/+}$) showed no myeloid cell enrichment, whereas the control chimeras with NLRP3 expression in the hematopoietic compartment (NLRP3$^{+/+}$ → NLRP3$^{+/+}$) exhibited myeloid cell accumulation (**Fig. 7C**). The above results indicate that NLRP3 expression in hematopoietic cells is critical for *P. gingivalis*–induced colorectal cancer development.

## Discussion

In addition to its role as a keystone pathogen in chronic periodontitis, P. gingivalis was found to be closely related to orodigestive cancer, and its tumorigenesis mechanism has been broadly studied (29).

**Figure 5.**

*P. gingivalis* changes the tumor immune environment by selectively expanding myeloid-derived immune cells and inducing a proinflammatory microenvironment. **A,** A schematic gating strategy for the identification of various tumor-infiltrating immune cell subsets in a rectal xenograft model. **B,** The cell number per gram of tissue is shown for CD11b$^+$ myeloid cells, CD11b$^+$MHC II$^+$ myeloid cells, DCs, and macrophages in the treatment groups. BHI broth was used as a control. Each symbol represents the data from an individual mouse. **C,** Representative image of immunofluorescence staining and CD11b$^+$ cell counting per 400× field. Arrows, CD11b$^+$ cells that infiltrate the tissue. **D,** The mRNA and protein levels of TNFα, IL6, and IL1β in cells derived from tumors extracted from submucosal model mice and the culture supernatants were detected by qPCR and ELISA, respectively. **E,** RNA sequencing was conducted, and heatmaps of selected genes related to immune cell recruitment and response that responded to *P. gingivalis* stimulation and relationships between *P. gingivalis*–infected tumors and the expression of inflammatory cytokines were established. **F,** The relative mRNA expression and supernatant concentration of TNFα, IL6, and IL1β in THP1 cells stimulated with *P. gingivalis* ATCC 33277 for 3, 6, 12, and 24 hours were detected by qPCR and ELISA, respectively. The mean percentage ± SEM is shown. *, $P < 0.05$; **, $P < 0.01$; ***, $P < 0.001$ by Student *t* test; N.S., not significant; one representative experiment of two replicates is shown.

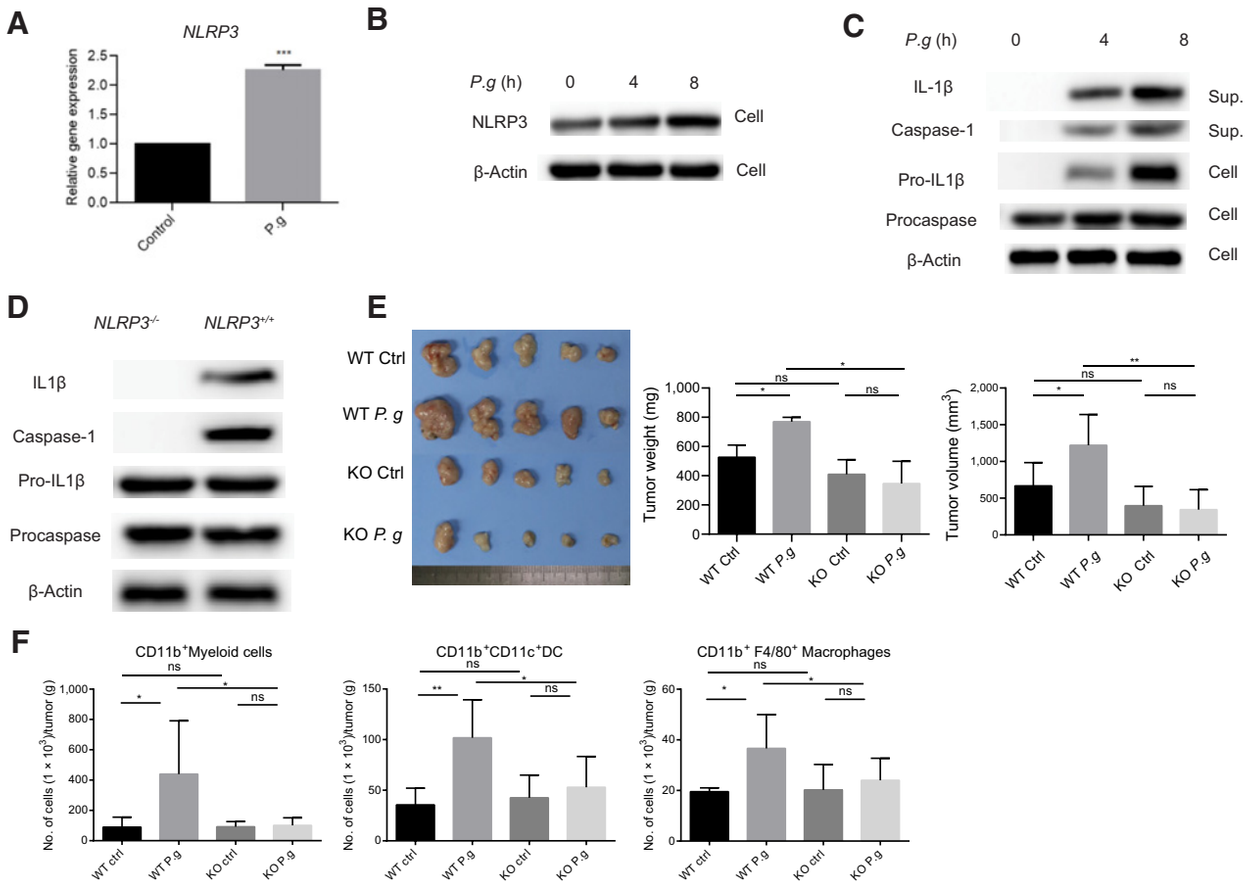


**Figure 6.**

*P. gingivalis* can activate the NLRP3 inflammasome *in vitro* but fails to induce colorectal tumor growth in NLRP3$^{-/-}$ mice. **A,** The expression of the NLRP3 inflammasome in individual CD45$^{+}$ cells derived from tumors from submucosal model mice was detected by qPCR. **B,** BMDMs were cocultured with *P. gingivalis* for 4 and 8 hours, and protein was extracted from BMDMs for Western blot detection of NLRP3 expression. **C,** *P. gingivalis* was cocultured with BMDMs for 4 and 8 hours, after which, pro-IL1β and procaspase-1 levels in cells and IL1β and caspase-1 levels in culture supernatant were detected. **D,** *P. gingivalis* was cocultured with NLRP3$^{-/-}$ BMDMs or WT BMDMs for 8 hours, after which, the cells were assessed for procaspase-1 expression, whereas the cell culture supernatant was assessed for IL1β and caspase-1 levels. **E,** Representative *in situ* image showing MC38 tumors from WT or NLRP3$^{-/-}$ submucosal model mice subjected to oral gavage of *P. gingivalis* or BHI broth. The tumor weight and volume of each group are shown. **F,** The cell number per gram of tissue is shown for CD11b$^{+}$ myeloid cells, DCs, and macrophages in the treatment groups. The mean percentage ± SEM is shown. *, $P < 0.05$; **, $P < 0.01$; ***, $P < 0.001$ by Student *t* test; ns, not significant; one representative experiment is shown; the experiment was performed in triplicate.

*P. gingivalis* can stimulate oral squamous cell carcinoma (OSCC) tumorigenesis by promoting the expression of key molecules in tumorigenesis, such as cyclin D1 and matrix metalloproteinase-9 (MMP9; refs. 30, 31). Persistent exposure to *P. gingivalis* induced morphological changes in cells, increased the proliferation ability of cells as indicated by a higher S-phase fraction, and promoted cell migration and invasion in OSCC (32). Our previous work also revealed that *P. gingivalis* promotes the proliferation of colorectal cancer cells by activating the MAPK/ERK signaling pathway (33). In this study, our results demonstrate that *P. gingivalis* can recruit tumor-infiltrating myeloid cells, activate the NLRP3 inflammasome and generate a proinflammatory microenvironment, all of which are conducive to the progression of colorectal neoplasms.

Accumulating evidence indicates that oral microbes are closely associated with colorectal cancer (34). Expansion of the oral microbiota during periodontitis is reported to promote colitis via colonization of the gut as well as induction of migratory immune cells (35). *F. nucleatum*, another keystone periodontal pathogen, has been shown to be enriched in colorectal cancer and promote colorectal carcinogenesis (5–7, 36–39). *P. gingivalis*, which often coexists with *F. nucleatum* in dental biofilms, was recently reported to have a higher positive rate in fecal samples from patients with colorectal cancer than in samples from normal subjects (40). Recently, *P. gingivalis* was also found to be enriched in esophageal squamous carcinoma tissue and the feces of patients with colorectal cancer (10, 19). However, whether *P. gingivalis* is localized in cancerous colonic tissues and whether it plays a role in colorectal carcinogenesis have not been confirmed. Our results showed that in patients with colorectal cancer, *P. gingivalis* was enriched in cancer tissues. A high abundance of *P. gingivalis* was associated with poorer OS and RFS in patients with colorectal cancer from both cohorts compared with the OS and RFS of patients with low abundance. Our study confirmed for the first time the

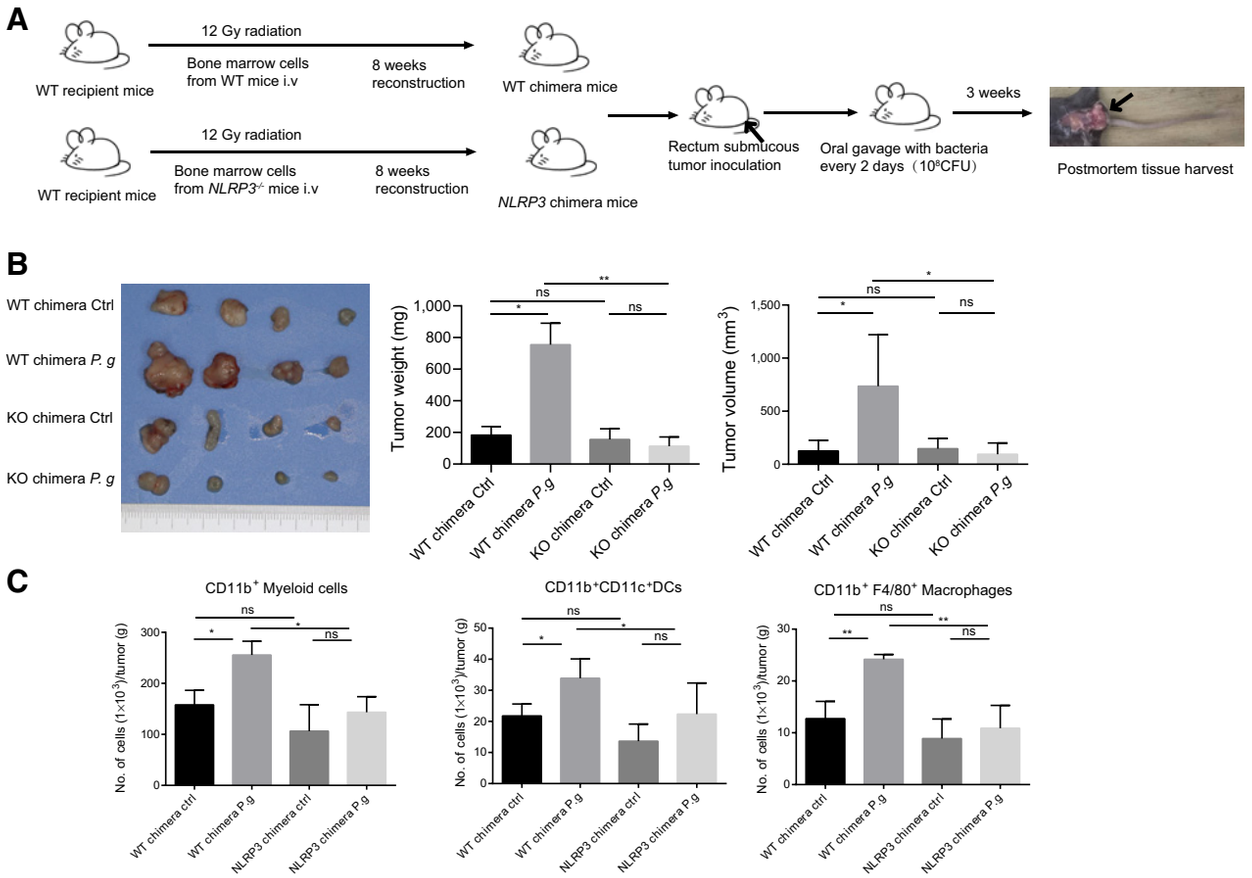


**Figure 7.**

*P. gingivalis* promotes colorectal tumorigenesis by activating the NLRP3 inflammasome in hematopoietic compartments. **A,** Schematic diagram of the submucosal MC38 tumor model in chimeric mice. Recipient WT mice were lethally irradiated with a total dose of 12 Gy, followed by BM reconstitution with BM cells from NLRP3$^{-/-}$ or control mice. After 8 weeks of recovery, an orthotopic colorectal xenograft mouse model was generated. **B,** A representative *in situ* image showing MC38 tumors from WT chimera or NLRP3$^{-/-}$ chimera mice subjected to oral gavage of *P. gingivalis* or BHI broth. The tumor weight and volume of each group are shown. **C,** The cell number per gram of tissue is shown for CD11b$^{+}$ myeloid cells, DCs, and macrophages in the treatment groups. The mean percentage ± SEM is shown; *, $P < 0.05$; **, $P < 0.01$ by Student *t* test; ns, not significant; one representative data of three is depicted.

localization and invasive behavior of *P. gingivalis* in cancerous tissue and the effects of *P. gingivalis* on tumor progression and prognosis in patients with colorectal cancer.

Bacterially driven mouse models of intestinal tumorigenesis have been used to confirm the contributions of bacteria to tumor progression (41, 42). To investigate the early and advanced stages, $Apc^{Min/+}$ mice and subcutaneous and orthotopic rectal cancer models were utilized, and the results showed that *P. gingivalis* plays an important role in the initiation and development of colorectal cancer. *P. gingivalis* has a number of virulence factors that can drive immune escape, including dampening host immunity, altering cytokine production, and affecting cell signaling mechanisms (43). The inflammatory response initiated by *P. gingivalis* in periodontitis includes the modulation of CD11b$^{+}$ cell functions (44–46), degradation of complement fragments (47) and recruitment of host regulatory proteins (Factor H, C4 binding protein). In our study, we observed a markedly increased number of CD11b$^{+}$ myeloid cells in tumor sites in mice infected with *P. gingivalis* compared with uninfected mice. Myeloid cells are reported to be associated with tumor progression, angiogenesis, and the modulation of antitumor immunity (48–51). RNA sequencing also revealed that the levels of multiple inflammatory cytokines were elevated in the *P. gingivalis* group. We noticed increased expression of the proinflammatory cytokines IL1β, IL6, and TNFα, which positively affect tumor growth, invasion and metastasis (52). Serum IL1β, IL6, and TNFα levels have also been found to be related to the poor prognosis of colorectal cancer (53). We confirmed that *P. gingivalis* infection promoted IL1β, IL6, and TNFα release from myeloid cells (THP1 cells) *in vitro* and that these cytokines were found in the culture supernatants of single-cell suspensions derived from tumors. These findings suggest that alterations in the immune microenvironment characterized by the release of the proinflammatory molecules IL1β, IL6, and TNFα from myeloid cells are the potential underlying cause of *P. gingivalis*–induced tumorigenesis and the associated poor colorectal cancer prognosis.

NLRP3 has been analyzed extensively in its contribution to colitis and has been shown to be associated with the development of colitis-

associated colorectal cancer (54). Several studies have revealed the mechanisms by which *P. gingivalis* can activate the NLRP3 inflammasome (55). The lipopolysaccharide of *P. gingivalis* is a virulence factor that induces NLRP3 activation in periodontal ligament fibroblasts (56). Myeloid cells stimulated with extracellular vesicles released from *P. gingivalis* produce large amounts of inflammatory mediators and activate the inflammasome and pyroptotic cell death pathways (57). Two common colorectal cancer–associated microbes, *F. nucleatum* and *B. fragilis*, have been reported to activate the NLRP3 inflammasome in several cell types (58, 59). However, evidence regarding the association of microbe-mediated NLRP3 activation and colorectal cancer development is lacking. It is widely believed that exotic components of commensal flora can trigger an abnormal innate immune response from local myeloid cells. Our results show that the release of IL1β was higher than that of IL6 and TNFα. NLRP3 expression was elevated in $CD45^+$ tumor-infiltrating immune cells in the *P. gingivalis* group, which indicates an active NLRP3 status. The role of innate immune signaling in intestinal inflammation has only recently begun to be elucidated. Several members of the cytosolic NLR family have been identified as key regulators of cytokine production. Our *in vitro* study revealed that *P. gingivalis* could activate the NLRP3 inflammasome and IL1β secretion and elicit tumor-promoting effects in WT mice and WT chimeras but could not promote colorectal cancer progression in either *NLRP3*$^{-/-}$ mice or *NLRP3*-deficient chimeric mice, as shown in **Figs. 3** and **7**. These data strongly suggest that *P. gingivalis*–driven activation of the hematopoietic NLRP3 inflammasome underlies the severity of colorectal cancer progression in mice. We found that *P. gingivalis* significantly enhances inflammation, as indicated by increases in IL1β release and myeloid cell infiltration, which suggests that exposure to *P. gingivalis* affects processes involved in inflammatory disorders and the promotion of colorectal cancer.

In summary, our results demonstrate that *P. gingivalis* is associated with a poor prognosis in human colorectal cancer because this bacterium colonizes and becomes enriched in tumor tissue, resulting in activation of the NLRP3 inflammasome in the immune microenvironment, which ultimately promotes colorectal carcinoma progression. Targeted reduction in *P. gingivalis* populations in the oral cavity, where *P. gingivalis* is most abundant, or in the gut may be an accessible means of reducing tumor development and progression. However, there are some limitations in the study. There was no exploration of the effect of *P. gingivalis* on genetic and molecular changes within the tumor microenvironment. Future work will address whether *P. gingivalis* can promote colorectal cancer by directly interacting with host cancer cells, secreting oncogenic virulence factors or generating carcinogenic microbial metabolites; these studies will better define the passenger/driver role of *P. gingivalis* in the pathogenesis of colorectal cancer. The effect of *P. gingivalis* within the broad microbial environment should also be further studied to confirm the role of *P. gingivalis* in the etiology of colorectal cancer.

## Authors' Disclosures

G. Zeng reports grants from National Natural Science Foundation of China (NSFC) during the conduct of the study, as well as other support from Revaissant Bioscience outside the submitted work. No disclosures were reported by the other authors.

## Authors' Contributions

**X. Wang:** Formal analysis, investigation, writing–original draft, writing–review and editing. **Y. Jia:** Data curation, validation, investigation. **L. Wen:** Validation, investigation, writing–review and editing. **W. Mu:** Investigation. **X. Wu:** Resources, methodology. **T. Liu:** Formal analysis, investigation. **X. Liu:** Data curation, validation. **J. Fang:** Validation. **Y. Luan:** Data curation, software. **P. Chen:** Resources. **J. Gao:** Resources, methodology. **K.-A. Nguyen:** Resources, methodology. **J. Cui:** Supervision, visualization. **G. Zeng:** Visualization, methodology. **P. Lan:** Resources, supervision. **Q. Chen:** Supervision. **B. Cheng:** Supervision, funding acquisition. **Z. Wang:** Conceptualization, supervision, writing–original draft, writing–review and editing.

## Acknowledgments

This project was supported by the National Natural Science Foundation of China (grant no. 81630025 to B. Cheng; nos. 81772896 and 81972532 to Z. Wang; and nos. 81991500 and 81991502 to Q. Chen).

The costs of publication of this article were defrayed in part by the payment of page charges. This article must therefore be hereby marked *advertisement* in accordance with 18 U.S.C. Section 1734 solely to indicate this fact.

Received November 17, 2020; revised February 11, 2021; accepted March 16, 2021; published first March 18, 2021.

## References

1. Marchesi JR, Adams DH, Fava F, Hermes GD, Hirschfield GM, Hold G, et al. The gut microbiota and host health: a new clinical frontier. Gut 2016; 65:330–9.
2. Segata N, Haake SK, Mannon P, Lemon KP, Waldron L, Gevers D, et al. Composition of the adult digestive tract bacterial microbiome based on seven mouth surfaces, tonsils, throat and stool samples. Genome Biol 2012;13:R42.
3. Flemer B, Warren RD, Barrett MP, Cisek K, Das A, Jeffery IB, et al. The oral microbiota in colorectal cancer is distinctive and predictive. Gut 2018;67: 1454–63.
4. Hashemi Goradel N, Heidarzadeh S, Jahangiri S, Farhood B, Mortezaee K, Khanlarkhani N, et al. Fusobacterium nucleatum and colorectal cancer: A mechanistic overview. J Cell Physiol 2019;234:2337–44.
5. Kostic AD, Chun E, Robertson L, Glickman JN, Gallini CA, Michaud M, et al. Fusobacterium nucleatum potentiates intestinal tumorigenesis and modulates the tumor-immune microenvironment. Cell Host Microbe 2013;14:207–15.
6. Yu T, Guo F, Yu Y, Sun T, Ma D, Han J, et al. Fusobacterium nucleatum promotes chemoresistance to colorectal cancer by modulating autophagy. Cell 2017;170: 548–63.
7. Abed J, Emgård JE, Zamir G, Faroja M, Almogy G, Grenov A, et al. Fap2 mediates Fusobacterium nucleatum colorectal adenocarcinoma enrichment by binding to tumor-expressed Gal-GalNAc. Cell Host Microbe 2016; 20:215–25.
8. Hajishengallis G, Abe T, Maekawa T, Hajishengallis E, Lambris JD. Role of complement in host-microbe homeostasis of the periodontium. Semin Immunol 2013;25:65–72.
9. Ahn J, Segers S, Hayes RB. Periodontal disease, Porphyromonas gingivalis serum antibody levels and orodigestive cancer mortality. Carcinogenesis 2012;33:1055–8.
10. Sinha R, Ahn J, Sampson JN, Shi J, Yu G, Xiong X, et al. Fecal microbiota, fecal metabolome, and colorectal cancer interrelations. PLoS One 2016;11:e0152126.
11. Purcell RV, Visnovska M, Biggs PJ, Schmeier S, Frizelle FA. Distinct gut microbiome patterns associate with consensus molecular subtypes of colorectal cancer. Sci Rep 2017;7:11590.
12. Abraham SN, St John AL. Mast cell-orchestrated immunity to pathogens. Nat Rev Immunol 2010;10:440–52.
13. Próchnicki T, Latz E. Inflammasomes on the crossroads of innate immune recognition and metabolic control. Cell Metab 2017;26:71–93.
14. Belibasakis GN, Guggenheim B, Bostanci N. Down-regulation of NLRP3 inflammasome in gingival fibroblasts by subgingival biofilms: involvement of Porphyromonas gingivalis. Innate Immun 2013;19:3–9.
15. Taxman DJ, Swanson KV, Broglie PM, Wen H, Holley-Guthrie E, Huang MT, et al. Porphyromonas gingivalis mediates inflammasome repression in polymicrobial cultures through a novel mechanism involving reduced endocytosis. J Biol Chem 2012;287:32791–9.

16. Yamaguchi Y, Kurita-Ochiai T, Kobayashi R, Suzuki T, Ando T. Activation of the NLRP3 inflammasome in Porphyromonas gingivalis-accelerated atherosclerosis. Pathog Dis 2015;73:ftv011.
17. Yoshida K, Okamura H, Hiroshima Y, Abe K, Kido JI, Shinohara Y, et al. PKR induces the expression of NLRP3 by regulating the NF-κB pathway in Porphyromonas gingivalis-infected osteoblasts. Exp Cell Res 2017;354:57–64.
18. Kolodkin-Gal D, Edden Y, Hartshtark Z, Ilan L, Khalaileh A, Pikarsky AJ, et al. Herpes simplex virus delivery to orthotopic rectal carcinoma results in an efficient and selective antitumor effect. Gene Ther 2009;16:905–15.
19. Gao S, Li S, Ma Z, Liang S, Shan T, Zhang M, et al. Presence of Porphyromonas gingivalis in esophagus and its association with the clinicopathological characteristics and survival in patients with esophageal cancer. Infect Agents Cancer 2016;11:3.
20. Castellarin M, Warren RL, Freeman JD, Dreolini L, Krzywinski M, Strauss J, et al. Fusobacterium nucleatum infection is prevalent in human colorectal carcinoma. Genome Res 2012;22:299–306.
21. Saeliw T, Tangsuwansri C, Thongkorn S, Chonchaiya W, Suphapeetiporn K, Mutirangura A, et al. Integrated genome-wide Alu methylation and transcriptome profiling analyses reveal novel epigenetic regulatory networks associated with autism spectrum disorder. Mol Autism 2018;9:27.
22. Tanabe M, Kanehisa M. Using the KEGG database resource. Curr Protoc Bioinformatics 2012;Chapter 1:Unit1.12.
23. Magoc T, Salzberg SL. FLASH: fast length adjustment of short reads to improve genome assemblies. Bioinformatics 2011;27:2957–63.
24. Segata N, Izard J, Waldron L, Gevers D, Miropolsky L, Garrett WS, et al. Metagenomic biomarker discovery and explanation. Genome Biol 2011;12:R60.
25. Brenner H, Kloor M, Pox CP. Colorectal cancer. Lancet 2014;383:1490–502.
26. Moser AR, Luongo C, Gould KA, McNeley MK, Shoemaker AR, Dove WF. ApcMin: a mouse model for intestinal and mammary tumorigenesis. Eur J Cancer 1995;31a:1061–4.
27. Song W, Shen L, Wang Y, Liu Q, Goodwin TJ, Li J, et al. Synergistic and low adverse effect cancer immunotherapy by immunogenic chemotherapy and locally expressed PD-L1 trap. Nat Commun 2018;9:2237.
28. Kaakoush NO. Insights into the role of Erysipelotrichaceae in the human host. Front Cell Infect Microbiol 2015;5:84.
29. Olsen I, Yilmaz Ö. Possible role of Porphyromonas gingivalis in orodigestive cancers. J Microbiol 2019;11:1563410.
30. Inaba H, Sugita H, Kuboniwa M, Iwai S, Hamada M, Noda T, et al. Porphyromonas gingivalis promotes invasion of oral squamous cell carcinoma through induction of proMMP9 and its activation. Cell Microbiol 2014;16:131–45.
31. Chang C, Wang H, Liu J, Pan C, Zhang D, Li X, et al. Porphyromonas gingivalis infection promoted the proliferation of oral squamous cell carcinoma cells through the miR-21/PDCD4/AP-1 negative signaling pathway. ACS Infect Dis 2019;5:1336–47.
32. Geng F, Liu J, Guo Y, Li C, Wang H, Wang H, et al. Persistent exposure to Porphyromonas gingivalis promotes proliferative and invasion capabilities, and tumorigenic properties of human immortalized oral epithelial cells. Front Cell Infect Microbiol 2017;7:57.
33. Mu W, Jia Y, Chen X, Li H, Wang Z, Cheng B. Intracellular Porphyromonas gingivalis promotes the proliferation of colorectal cancer cells via the MAPK/ERK signaling pathway. Front Cell Infect Microbiol 2020;10:584798.
34. Koliarakis I, Messaritakis I, Nikolouzakis TK, Hamilos G, Souglakos J, Tsiaoussis J. Oral bacteria and intestinal dysbiosis in colorectal cancer. Int J Mol Sci 2019;20.
35. Kitamoto S, Nagao-Kitamoto H, Jiao Y, Gillilland MG 3rd, Hayashi A, Imai J, et al. The intermucosal connection between the mouth and gut in commensal pathobiont-driven colitis. Cell 2020;182:447–62.
36. Han YW. Fusobacterium nucleatum: a commensal-turned pathogen. Curr Opin Microbiol 2015;23:141–7.
37. Yang Y, Weng W, Peng J, Hong L, Yang L, Toiyama Y, et al. Fusobacterium nucleatum increases proliferation of colorectal cancer cells and tumor development in mice by activating toll-like receptor 4 signaling to nuclear factor-kappaB, and up-regulating expression of microRNA-21. Gastroenterology 2017;152:851–66.
38. Rubinstein MR, Baik JE, Lagana SM, Han RP, Raab WJ, Sahoo D, et al. Fusobacterium nucleatum promotes colorectal cancer by inducing Wnt/β-catenin modulator Annexin A1. EMBO Rep 2019;20:e47638.
39. Rubinstein MR, Wang X, Liu W, Hao Y, Cai G, Han YW. Fusobacterium nucleatum promotes colorectal carcinogenesis by modulating E-cadherin/β-catenin signaling via its FadA adhesin. Cell Host Microbe 2013;14:195–206.
40. Nakajima M, Arimatsu K, Kato T, Matsuda Y, Minagawa T, Takahashi N, et al. Oral administration of P. gingivalis induces dysbiosis of gut microbiota and impaired barrier function leading to dissemination of enterobacteria to the liver. PLoS One 2015;10:e0134234.
41. Wu S, Rhee KJ, Albesiano E, Rabizadeh S, Wu X, Yen HR, et al. A human colonic commensal promotes colon tumorigenesis via activation of T helper type 17 T cell responses. Nat Med 2009;15:1016–22.
42. Arthur JC, Perez-Chanona E, Muhlbauer M, Tomkovich S, Uronis JM, Fan TJ, et al. Intestinal inflammation targets cancer-inducing activity of the microbiota. Science 2012;338:120–3.
43. Hajishengallis G. Periodontitis: from microbial immune subversion to systemic inflammation. Nat Rev Immunol 2015;15:30–44.
44. Borgeson E, Lonn J, Bergstrom I, Brodin VP, Ramstrom S, Nayeri F, et al. Lipoxin A(4) inhibits Porphyromonas gingivalis-induced aggregation and reactive oxygen species production by modulating neutrophil-platelet interaction and CD11b expression. Infect Immun 2011;79:1489–97.
45. Papadopoulos G, Shaik-Dasthagirisaheb YB, Huang N, Viglianti GA, Henderson AJ, Kantarci A, et al. Immunologic environment influences macrophage response to Porphyromonas gingivalis. Mol Oral Microbiol 2017;32:250–61.
46. Su L, Xu Q, Zhang P, Michalek SM, Katz J. Phenotype and function of myeloid-derived suppressor cells induced by Porphyromonas gingivalis infection. Infect Immun 2017;85:e00213–17.
47. Maekawa T, Krauss JL, Abe T, Jotwani R, Triantafilou M, Triantafilou K, et al. Porphyromonas gingivalis manipulates complement and TLR signaling to uncouple bacterial clearance from inflammation and promote dysbiosis. Cell Host Microbe 2014;15:768–78.
48. Coussens LM, Pollard JW. Leukocytes in mammary development and cancer. Cold Spring Harb Perspect Biol 2011;3:a003285.
49. Galdiero MR, Marone G, Mantovani A. Cancer inflammation and cytokines. Cold Spring Harb Perspect Biol 2018;10:a028662.
50. Mantovani A, Cassatella MA, Costantini C, Jaillon S. Neutrophils in the activation and regulation of innate and adaptive immunity. Nat Rev Immunol 2011;11:519–31.
51. Qian BZ, Pollard JW. Macrophage diversity enhances tumor progression and metastasis. Cell 2010;141:39–51.
52. Ray AL, Berggren KL, Restrepo Cruz S, Gan GN, Beswick EJ. Inhibition of MK2 suppresses IL-1beta, IL-6, and TNF-alpha-dependent colorectal cancer growth. Int J Cancer 2018;142:1702–11.
53. Chang PH, Pan YP, Fan CW, Tseng WK, Huang JS, Wu TH, et al. Pretreatment serum interleukin-1beta, interleukin-6, and tumor necrosis factor-alpha levels predict the progression of colorectal cancer. Cancer Med 2016;5:426–33.
54. Ahechu P, Zozaya G, Martí P, Hernández-Lizoáin JL, Baixauli J, Unamuno X, et al. NLRP3 inflammasome: a possible link between obesity-associated low-grade chronic inflammation and colorectal cancer development. Front Immunol 2018;9:2918.
55. Ding PH, Yang MX, Wang NN, Jin LJ, Dong Y, Cai X, et al. Porphyromonas gingivalis-induced NLRP3 inflammasome activation and its downstream interleukin-1β release depend on caspase-4. Front Microbiol 2020;11:1881.
56. Lian D, Dai L, Xie Z, Zhou X, Liu X, Zhang Y, et al. Periodontal ligament fibroblasts migration injury via ROS/TXNIP/Nlrp3 inflammasome pathway with Porphyromonas gingivalis lipopolysaccharide. Mol Immunol 2018;103:209–19.
57. Fleetwood AJ, Lee MKS, Singleton W, Achuthan A, Lee MC, O'Brien-Simpson NM, et al. Metabolic remodeling, inflammasome activation, and pyroptosis in macrophages stimulated by Porphyromonas gingivalis and its outer membrane vesicles. Front Cell Infect Microbiol 2017;7:351.
58. Bui FQ, Johnson L, Roberts J, Hung SC, Lee J, Atanasova KR, et al. Fusobacterium nucleatum infection of gingival epithelial cells leads to NLRP3 inflammasome-dependent secretion of IL-1β and the danger signals ASC and HMGB1. Cell Microbiol 2016;18:970–81.
59. Yang PC, Li XJ, Yang YH, Qian W, Li SY, Yan CH, et al. The influence of Bifidobacterium bifidum and Bacteroides fragilis on enteric glial cell-derived neurotrophic factors and inflammasome. Inflammation 2020;43:2166–77.